Available online at www.sciencedirect.com
SCIENCE DIRECT®
Optics Communications 228 (2003) 91–98
OPTICS COMMUNICATIONS
www.elsevier.com/locate/optcom

Characteristics of optical bandpass filters employing series-cascaded double-ring resonators ☆

Jianyi Yang [a,b,*], Qingjun Zhou [b], Feng Zhao [b], Xiaoqing Jiang [a], Brie Howley [b], Minghua Wang [a], Ray T. Chen [b]

[a] Department of Information Science and Electronics Engineering, Zhejiang University, 38 ZheDa Rd., Hangzhou 310027, China
[b] Microelectronics Research Center/Department of Electrical and Computer Engineering, University of Texas at Austin, Austin, TX 78758, USA

Received 26 June 2003; received in revised form 25 September 2003; accepted 26 September 2003

Abstract

The filtering characteristics of a series-cascaded double-ring optical resonator (SDRR) are investigated. The roles of coupling coefficients and the effects of optical loss are analyzed. The relationships of the coupling coefficients with the characteristics of the SDRR filter are expressed with simple analytical formulas. With the derived approximate formulas, it is found that the bandwidth ratio of the SDRR filter is mainly dependent on the shape factor defined in this paper. The performance of the SDRR filter, especially the bandwidth ratio, is improved significantly in comparison with that of the single-ring-resonator filter. The analytical results also indicate that the optical loss in the microrings has a strong influence on the characteristics of the SDRR filter.

Keywords: Integrated optics; Optical filter; Optical waveguide; Optical microring resonator

1. Introduction

With recent advances in planar fabrication techniques, there has been an increased interest in microring-based optical waveguide resonators [1–7]. A lot of work has been performed on optical filters incorporating waveguide microrings as the building block elements [3–5,8–15]. Since the single-ring-resonator (SRR) filter has a simple Lorentzian response, high-order multiple-ring-resonator (MRR) filters, which can be realized in either a serial or parallel cascade configuration [8–15], were proposed to achieve flat-top, fast-rolloff, and large-stopband-rejection filtering bands. In Little's recent report [15], MRRs fabricated on the glass material called Hydex™ with low-insertion loss and box-like responses were reported. These high-order filters, however, require tight

☆ This work is supported in part by the Major State Basic Research Development Program under the contract G1999033104 and by the National Natural Science Foundation under the contracts 69907004, 60177012 and 60277034.
* Corresponding author. Tel.: +8657187952867; fax: +8657187952867.
E-mail address: yangjy@zju.edu.cn (J. Yang).

0030-4018/$ - see front matter © 2003 Elsevier B.V. All rights reserved.
doi:10.1016/j.optcom.2003.09.092

fabrication control to ensure coincident resonances in all microrings and accurate power coupling coefficients of all coupling regions. Many methods, such as the coupled-mode method [8] and the transfer-matrix method [9,11], have been employed to analyze the characteristics of microring-based optical filters. An approach to synthesize high-order optical filters has also been proposed [8,11]. However, to our knowledge, except for the SRR filter, no published study has quantitatively explained the exact roles all coupling coefficients play in determining the bandwidth, the bandwidth ratio, and the stopband rejection, and the possible effects optical loss makes on the characteristics of the MRR filter.

The aim of this paper is to explore the feasibility of employing a series-cascaded double-ring resonator (SDRR) to realize a high-performance optical filter. One of the advantages of this second-order microring-based optical filter is that it has the simplest structure among high-order filters, and thus its fabrication is much easier and more practical. Meanwhile, the size of the SDRR filter is kept small, which is the key feature of the microring-based optical component for high-density optical integration. In this paper, the roles of coupling coefficients and the effects of optical loss are analyzed and formulated for the SDRR filter. With the derived formulas, we can easily set and/or tune the bandwidth ratio of the SDRR, which mainly depends on the shape factor defined in the following sections, as well as the bandwidth. This makes designing high-performance SDRR filters simple and is very useful to guide trimming in the fabrication of SDRR filters. We calculated the bandwidth ratio of the filtering band and found that the band shape of the SDRR filter is much better than that of the SRR filter.

The paper is organized as follows. In Section 2, the transfer function of the SDRR bandpass filter is presented. Based on the transfer function, in Section 3, the formulas for the filtering characteristics are derived. The performance of the SDRR filter is compared with that of the SRR filter. The influence of optical loss on the filtering characteristics is also investigated in Section 3. The results are summarized in Section 4.

2. Transfer function

The schematic diagram of the SDRR optical filter is depicted in Fig. 1. It consists of two mutually coupled waveguide microrings (Ring 1 and Ring 2) and two tangential straight waveguides (the bus and the dropping channels) that serve as evanescent wave input and output couplers. All waveguides are monomode. The two rings are identical and have the same free spectral range (FSR). Using the transfer-matrix method [11], we get the transfer function of the SDRR bandpass filter at the dropping channel:

$$D(\theta) = \frac{\mathrm{j}L_1^{1/2}L_2^{1/2}K_1K_2K_3\exp(-\mathrm{j}\theta)}{1-(L_1T_1T_2+L_2T_3T_2)\exp(-\mathrm{j}\theta)+L_1L_2T_1T_3\exp(-\mathrm{j}2\theta)}, \quad (1)$$

where, K_1 and K_3 are the two into-/out-of-ring amplitude coupling coefficients and K_2 is the ring-to-ring amplitude coupling coefficient, as shown in Fig. 1. $T_i^2 = 1 - K_i^2$ $(i = 1, 2, 3)$. $L_i = \exp(-\pi\alpha_i R)$ $(i = 1, 2)$ is the round-trip amplitude attenuation in Ring i, where α_i is the power loss coefficient of Ring i and R is the radius of both rings. θ is defined as the normalized frequency:

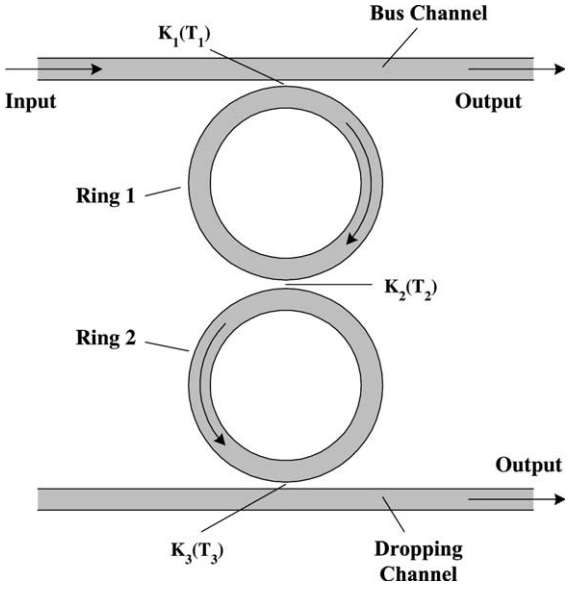

Fig. 1. Schematic diagram of the optical filter employing the series-cascaded double-ring resonator (SDRR).

$$\theta = \frac{2\pi v}{\mathrm{FSR}_v}, \tag{2}$$

i.e., the phase delay of the light with a frequency v in a round trip of a single waveguide ring. FSR_v is the FSR in the frequency domain. Since the transfer function $D(\theta)$ is periodic, we just need to analyze the characteristics in the period of $(-\pi, \pi)$.

3. Characteristic analysis

In this section, we first consider the case that the optical loss in the microrings can be ignored, and the two into-/out-of-ring amplitude coupling coefficients K_1 and K_3 are set identical. The influence of optical loss is analyzed later.

3.1. The resonances

In the case $L_1 = L_2 = 1$, the intensity transfer function of the SDRR filter can be obtained from Eq. (1) as follows:

$$|D(\theta)|^2 = \frac{(K_1K_2K_3)^2}{|1-(T_1T_2+T_3T_2)\exp(-\mathrm{j}\theta)+T_1T_3\exp(-\mathrm{j}2\theta)|^2}. \tag{3a}$$

Fig. 2 illustrates the dependence of the intensity transfer function on the normalized frequency in one period of the normalized frequency. In the curve of $K_2^2 = 0.01$ or $K_2^2 = 0.1$, there are two points giving the peak response. The two points correspond to the two resonances. It means that every resonant point of a single ring is split into two when this ring is set coupled with another identical ring. From Eq. (3a), it can be derived that the response at the resonance can reach its maximum value 1 only when $K_3 = K_1$. In the condition of $K_3 = K_1$, the intensity of transfer function becomes:

$$|D(\theta)|^2 = \frac{K_1^4K_2^2}{|1-2T_1T_2\exp(-\mathrm{j}\theta)+T_1^2\exp(-\mathrm{j}2\theta)|^2}. \tag{3b}$$

The normalized resonant frequencies θ_{res} is determined by the following equation:

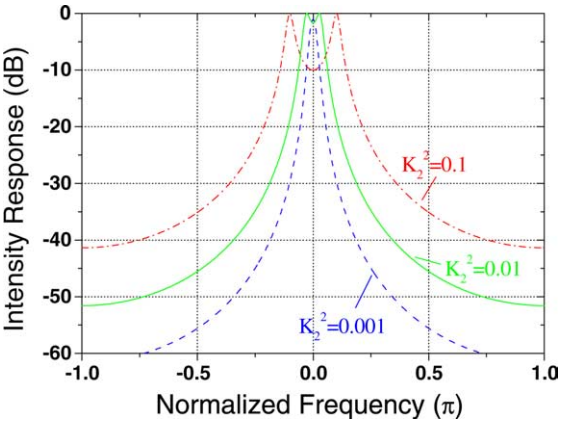

Fig. 2. Typical intensity responses of the bandpass SDRR filter. The employed parameters: $K_1^2 = K_3^2 = 0.1$.

$$\cos\theta_{\mathrm{res}} = \frac{1+T_1^2}{2T_1}T_2. \tag{4}$$

From Eq. (4), we know that the two resonances are degenerate only when $T_2 < 2T_1/(1+T_1^2)$. If $T_2 \geqslant 2T_1/(1+T_1^2)$, which also means:

$$K_2 \leqslant \frac{K_1^2}{2-K_1^2} \tag{5a}$$

the two resonant frequencies will merge back into the zero point $\theta = 0$ and the response at the resonance will decrease as K_2 decreases, as shown in Fig. 2.

When K_2 is large enough to support the two degenerate resonances, as is seen from the curves of $K_2^2 = 0.01$ and $K_2^2 = 0.1$ in Fig. 2, the intensity response has a minimum at $\theta = 0$ in the range between the two resonant frequencies. For a bandpass filter, it is commonly required that the ripple of the passband response should be minimized to an acceptable value. Thus, for the SDRR filter, the response $|D(\theta)|^2$ at $\theta = 0$ should be above a certain value ζ_0. For example, ζ_0 is about 0.9 if the ripple is required to be below 0.5 dB. Since generally $K_i^2 \ll 1$ $(i = 1, 2)$, to meet the condition $|D(0)|^2 \geqslant \zeta_0$ it can be derived from Eq. (3b) that K_2 must be in the following range:

$$\frac{1-\sqrt{1-\zeta_0}}{\sqrt{\zeta_0}}\frac{K_1^2}{2-K_1^2} \leqslant K_2 \leqslant \frac{1+\sqrt{1-\zeta_0}}{\sqrt{\zeta_0}}\frac{K_1^2}{2-K_1^2}. \tag{5b}$$

In fact, Eq. (5b) includes the conditions that the two resonances are merged. Combining Eqs. (5a) and (5b), to satisfy both $|D(\theta_{\text{res}})|^2 = 1$ and $|D(0)|^2 \geqslant \zeta_0$, we find that the ring-to-ring coupling coefficient K_2 needs to be tuned as

$$K_2 = \rho \frac{K_1^2}{2 - K_1^2}, \tag{6}$$

where $\rho = (1 + \sqrt{1-\zeta})/\sqrt{\zeta}$. Here, we define a shape factor ζ, which can be used not only to indicate the response at $\theta = 0$, but also to control the bandwidth ratio as analyzed in Section 3.3. The shape factor ζ is in the range of $\zeta_0 \leqslant \zeta \leqslant 1$. Thus, if K_2 is controlled to be the value given by Eq. (6), we can obtain a good passband shape in which the two resonances are kept degenerate and the response at the zero point is ζ. It should be noted that K_2 is of the same order of magnitude as K_1^2. The resonant frequencies have the following approximate expression:

$$\theta_{\text{res}}^2 \approx \sin^2 \theta_{\text{res}} \approx \frac{K_2^2 - K_1^4/4}{1 - K_1^2} \approx \frac{(\rho^2 - 1)}{4} \frac{K_1^4}{T_1^2}. \tag{7}$$

Here, it is assumed that $K_1^2 \ll 1$.

3.2. The bandwidth

To analyze the bandwidth of the SDRR filter, we begin with the denominator in the right-hand side of Eq. (3b). For the normalized frequencies near the zero point, considering the two resonant frequencies expressed by Eq. (7), we can approximate the denominator $d(\theta)$ as:

$$d(\theta) \approx \left[\left(1 - K_1^2\right)\theta^2 - \left(K_2^2 - K_1^4/4\right)\right]^2 + K_1^4 K_2^2. \tag{8}$$

Since the bandwidth is generally far smaller than the FSR, from Eq. (8), the normalized bandwidth of the bandpass SDRR filter is given by:

$$\text{BW}_{1/\eta} = 2\left(\frac{\sqrt{\eta - 1}K_1^2 K_2 + K_2^2 - K_1^4/4}{1 - K_1^2}\right)^{1/2}. \tag{9}$$

Here, η is defined as the bandwidth factor and Eq. (9) gives the bandwidth in which the response is within $-10 \log \eta$ (dB) of the peak. With Eq. (6), the bandwidth from Eq. (9) can be rewritten as:

$$\text{BW}_{1/\eta} \approx \left(2\rho\sqrt{\eta - 1} + \rho^2 - 1\right)^{1/2} \frac{K_1^2}{T_1}. \tag{10}$$

Fig. 3 demonstrates that Eq. (10) is accurate enough to give the 1 dB ($1/\eta \approx 0.8$), 3 dB ($1/\eta \approx 0.5$), 20 dB ($1/\eta = 0.01$) and 30 dB ($1/\eta = 0.001$) bandwidths when K_1^2 is small. From Eq. (10), it can be found that the bandwidth of the SDRR filter is almost proportional to the power coupling coefficient K_1^2. With this bandwidth formula, it is very easy to calculate the bandwidth ratio which will be analyzed in the following section.

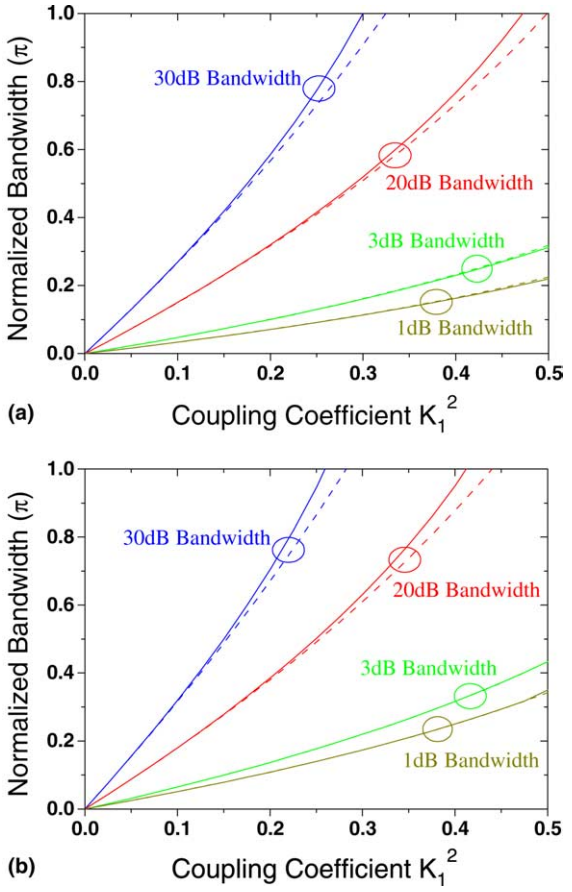

Fig. 3. Comparison between the approximate formula (11a) and (11b) and the accurate bandwidth values: (a) $\zeta = 1$ and (b) $\zeta = 0.9$. The solid line represents the accurate bandwidths; the dash line represents the bandwidths given by Eqs. (11a) and (11b).

3.3. Comparison with the SRR filter

In a bandpass filter, a large stopband rejection is critical to minimize crosstalk from neighboring signal channels. Here, we use the maximum extinction ratio $EX_{max} = 10\log(|D(\theta)|^2_{max}/|D(\theta)|^2_{min})$ (dB) to evaluate the stopband rejection and compare the difference between the SDRR filter and the SRR filter.For the SDRR filter, the peak response is at the resonant points:

$$|D(\theta)|^2_{max} = |D(\theta_{res})|^2 = 1 \tag{11a}$$

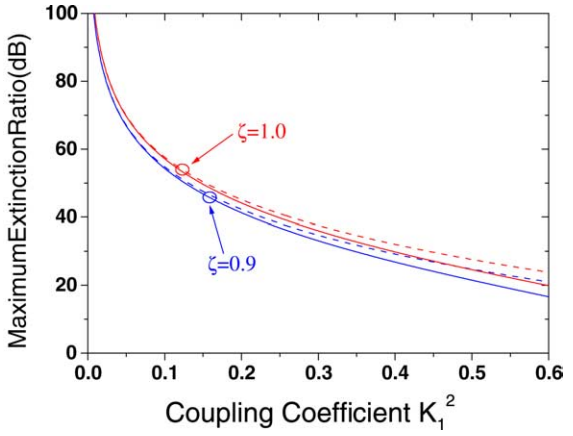

Fig. 4. Curves of the maximum extinction ratio versus the power coupling coefficient K_1^2. The solid line represents the accurate curves; the dash line represents the approximate curves given by Eq. (9).

and the minimum response is at the points $\theta = \pm\pi$:

$$|D(\theta)|^2_{min} = |D(\pm\pi)|^2 = \frac{K_1^4 K_2^2}{(1 + 2T_1T_2 + T_1^2)^2} \approx \rho^2 \frac{K_1^8}{64}, \tag{11b}$$

where the approximation can be obtained by assuming $K_1^2 \ll 1$. Thus the maximum extinction ratio of SDRR filter can be approximated by:

$$EX_{max} \approx 10\log\frac{64}{\rho^2 K_1^8}\ (\text{dB}). \tag{12}$$

Fig. 4 shows the curves of the maximum extinction ratio versus the power coupling coefficient K_1^2. It can be found that the maximum extinction ratio given by Eq. (12) is accurate if K_1^2 is small. Additionally, the maximum extinction ratio of the SRR filter is $EX_{max} \approx 10\log(4/K_1^4)$ [16] if its two into-/out-of-ring coupling coefficients are both small values of K_1 Since ρ cannot be larger than 2 (when ζ is 0.9, ρ is about 1.39), the maximum extinction ratio of the SDRR filter is more than twice that of the SRR filter. This means the SDRR filter can afford larger stopband rejection and lower crosstalk compared to the SRR filter.

The bandwidth ratio is another key property for a bandpass filter. When $\zeta = 1$, we have $\rho = 1$ and $BW_{1/\eta} = (2\sqrt{\eta - 1})^{1/2}(K_1^2/T_1)$ for the lossless SDRR filter according to the analysis in Section 3.2. Table 1 lists the bandwidth formulas of the

Table 1
Formulas of commonly defined bandwidths (normalized) of the SDRR ($\zeta = 1$) and SRR filters and ratios between them

Filter	$BW_{1/\eta}$	Formula	Bandwidth ratio		
			$BW_{1/\eta}/BW_{1\,dB}$	$BW_{1/\eta}/BW_{3\,dB}$	$BW_{1/\eta}/BW_{20\,dB}$
SDRR $\zeta = 1$	$BW_{1\,dB}$	$\frac{K_1^2}{T_1}$	1		
	$BW_{3\,dB}$	$\sqrt{2}\frac{K_1^2}{T_1}$	1.41	1	
	$BW_{20\,dB}$	$\sqrt{20}\frac{K_1^2}{T_1}$	4.47	3.16	1
	$BW_{30\,dB}$	$\sqrt{63.2}\frac{K_1^2}{T_1}$	7.95	5.62	1.78
SRR	$BW_{1\,dB}$	$\frac{K_1^2}{T_1}$	1		
	$BW_{3\,dB}$	$2\frac{K_1^2}{T_1}$	2	1	
	$BW_{20\,dB}$	$20\frac{K_1^2}{T_1}$	20	10	1
	$BW_{30\,dB}$	$63.2\frac{K_1^2}{T_1}$	63.2	31.6	3.16

SDRR ($\zeta = 1$) filter with various values of η and the ratios between them. The bandwidth formulas and the related bandwidth ratios of the SRR filter [16], in which the two into-/out-of-ring coupling coefficients are assumed to have the same value K_1 are also presented in Table 1 for comparison. It should be pointed out that the bandwidth ratios listed in Table 1 do not depend on the power coupling coefficient K_1^2 or any other parameter of the SDRR filter once ζ is chosen. Only when K_1^2 is not small enough and the approximation for Eqs. (8)–(10) is not accurate enough will the bandwidth ratio become larger. This is especially true for the ratio between the 1 dB (or 3 dB) and 20 dB (or 30 dB) bandwidths. Table 1 shows that the improvement of the band shape is significant if the SDRR is used as an optical filter instead of the SRR.

If the shape factor ζ of the SDRR filter is controlled to be smaller than 1, ρ becomes greater than 1 and the coefficient $(2\rho\sqrt{\eta-1}+\rho^2-1)^{1/2}$ in Eq. (10) increases. This increase of the coefficient $(2\rho\sqrt{\eta-1}+\rho^2-1)^{1/2}$ is greater for η of a smaller value (e.g., 1.25 or 2 for the 1 or 3 dB bandwidth, respectively) than that of a larger value (e.g., 100 or 1000 for the 20 or 30 dB bandwidth, respectively). Therefore, the decrease of ζ can result in the decrease of the bandwidth ratio and greater improvement of the band shape of the SDRR filter. Fig. 5 illustrates the changes of bandwidth ratios introduced by altering ζ. It should be noted that the decrease of ζ must meet the ripple requirement.

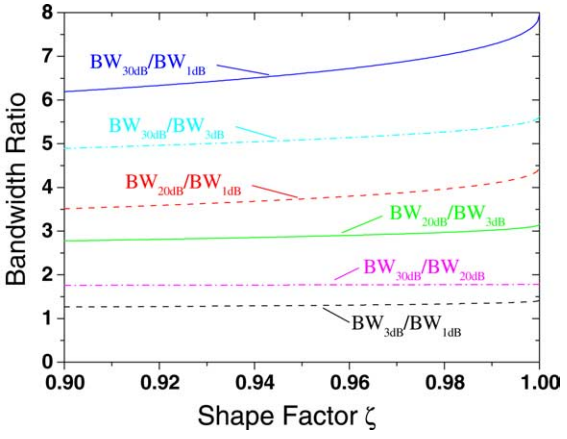

Fig. 5. Curves of the bandwidth ratios versus the shape factor ζ.

3.4. The influence of optical loss

The optical loss in microrings is unavoidable. It means we always have $L_1 < 1$ and $L_2 < 1$ for Eq. (1). Introducing the following definitions:

$$T_1'^2 = L_1 L_2 T_1 T_3, \tag{13a}$$

$$K_1'^2 = 1 - T_1'^2, \tag{13b}$$

$$\begin{cases} c_1 T_1' = L_1 T_1, \\ c_2 T_1' = L_2 T_3, \end{cases} \tag{13c}$$

$$\Gamma = \frac{c_1 + c_2}{2}, \tag{13d}$$

$$T_2' = \Gamma T_2, \tag{13e}$$

$$K_2'^2 = 1 - T_2'^2 \tag{13f}$$

we have the intensity transfer function of the bandpass SDRR filter from Eq. (1):

$$|D(\theta)|^2 = \frac{L_1 L_2 K_1^2 K_2^2 K_3^2}{K_1'^4 K_2'^2} \times \frac{K_1'^4 K_2'^2}{\left|1 - 2T_1' T_2' \exp(-\mathrm{j}\theta) + T_1'^2 \exp(-\mathrm{j}2\theta)\right|^2}. \tag{14}$$

The second term of the right-hand side of Eq. (14) is the intensity transfer function of a lossless SDRR filter, in which the two into-/out-of-ring coupling coefficients are both K_1' and the ring-to-ring coupling coefficient is K_2'. The first term is independent of the normalized frequency. Therefore, the influence of optical loss on the band shape is only presented by the second term and the first term gives the attenuation caused by optical loss. Eq. (14) can also be used to analyze the characteristics when K_3 is not set equal to K_1 in the lossless condition.

Fig. 6 demonstrates the change of the response given by the second term of the right-hand side of Eq. (14). As optical loss increases, the bandwidth ratio increases and the maximum extinction ratio decreases. However, the change of the bandwidth is little when optical loss is very small and the two resonances are still kept degenerate, which can be explained by Eqs. (6), (10) and (13a)–(13f). If optical loss is severe, for example $L^2 = 0.5$ as seen in Fig. 6, the band shape of the SDRR filter degrades dramatically.

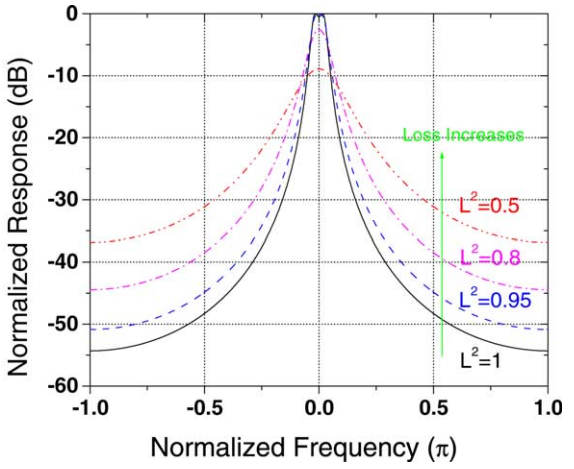

Fig. 6. Change of the band shape caused by optical loss. The employed parameters: $K_1^2 = K_3^2 = 0.1$ and $\zeta = 0.9$.

The bandwidth is much larger than expected, the bandwidth ratio is no longer as good as the data given in Table 1, the maximum extinction ratio is lower than −30 dB, and more attenuation of the response is introduced.

The main influence of optical loss is the attenuation of the output amplitude. Fig. 7 shows the influence of optical loss on the filtering response at the resonant frequency. We notice that even low loss will result in a rapid decrease of the output in the dropping channel.

If T_1 is given and T_3 is set to be $T_3 = T_1/(L_1L_2)$, the bus channel of the SDRR filter never has an output at the normalized frequencies given by the equation $\cos\theta = ((L_1^2 + T_1^2)/(2L_1T_1))T_2$. However, the filtered output from the dropping channel is far away from its maximum value, which can be reached by setting T_3 to the value around $L_1L_2T_1$. Assuming $L_1 = L_2 = L$, Fig. 7 compares the three cases that T_3 is controlled to be $T_3 = T_1/L^2$, $T_3 = T_1$, and $T_3 = L^2T_1$.

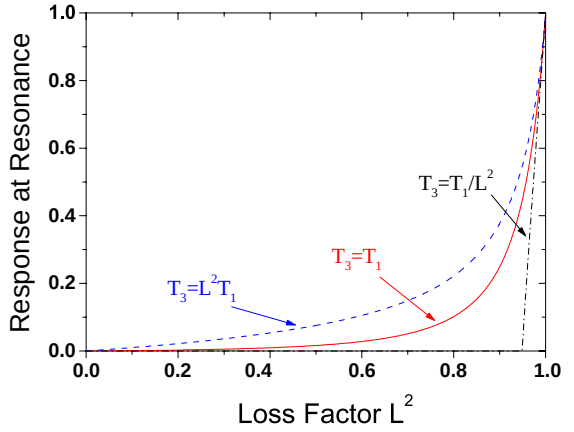

Fig. 7. Influence of optical loss on the output of the dropping channel at the resonant point. The employed parameters: $K_1^2 = 0.1$ and $\zeta = 1$.

4. Summary

In the above sections, the bandpass characteristics of the SDRR filter are studied in details. A set of analytical formulas is derived. These formulas give the relationship between the bandpass characteristics and the coupling coefficients, and can be employed to design high-performance SDRR filters. The analytical results indicate that the ring-to-ring coupling coefficient should follow Eq. (6) to generate a good band shape for the SDRR filter, and then the bandwidth is mainly determined by the into-/out-of-ring coupling coefficients. The Bandwidth ratio of the SDRR filter can be calculated very easily with a given shape factor ζ, and is almost independent of any other parameter of the SDRR filter. Compared to the characteristics of the SRR filter, those of the SDRR filter are improved significantly, especially the bandwidth ratio. The influence of the optical loss in microrings is also formulated and analyzed. To get a SDRR filter with good filtering performance, it is very important that the optical loss in microrings is controlled to be as low as possible. Otherwise, optical loss will not only cause serious attenuation of the bandpass response, but also lead to deterioration of the bandwidth ratio, the maximum extinction ratio, and even the bandwidth.

References

[1] J.P. Zhang, D.Y. Chu, S.L. Wu, S.T. Ho, W.G. Bi, C.W. Tu, R.C. Tiberio, Phys. Rev. Lett. 75 (14) (1995) 2678.
[2] M. Fujita, T. Baba, Appl. Phys. Lett. 80 (12) (2002) 2051.
[3] B. Little, J. Foresi, G. Steinmeyer, E. Thoen, S. Chu, H. Haus, E. Ippen, L. Kimerling, W. Greene, IEEE Photon. Technol. Lett. 10 (4) (1998) 549.
[4] J. Hryniewicz, P. Absil, B. Little, R. Wilson, P. Ho, IEEE Photon. Technol. Lett. 12 (3) (2000) 320.

[5] T. Kato, S. Suzuki, Y. Kokubun, CLEO/Pacific Rim 1 (2001) I_398.
[6] P. Rabiei, W. Steier, C. Zhang, L. Dalton, OFC TuF6 (2002) 31.
[7] H. Haus, C. Manolatou, OFC 3 (2000) 126.
[8] B. Little, S. Chu, H. Haus, J. Foresi, J. Laine, J. Lightwave Technol. 15 (6) (1997) 998.
[9] G. Griffel, IEEE Photon. Technol. Lett. 12 (7) (2000) 810.
[10] G. Griffel, IEEE Photon. Technol. Lett. 12 (12) (2000) 1642.
[11] R. Orta, P. Savi, R. Tascone, D. Trinchero, IEEE Photon. Technol. Lett. 7 (12) (1995) 1447.
[12] B. Little, S. Chu, J. Hryniewicz, P. Absil, Opt. Lett. 25 (5) (2000) 344.
[13] B. Little, S. Chu, W. Pan, D. Ripin, T. Kaneko, Y. Kokubun, E. Ippen, IEEE Photon. Technol. Lett. 11 (2) (1999) 215.
[14] S. Suzuki, Y. Hatakeyama, Y. Kokubun, S. Chu, J. Lightwave Technol. 20 (4) (2002) 745.
[15] B. Little, Advances in Microring Resonators, OSA Integrated Photonics Research Conference (IPR 2003), ITuE6, Jun. 2003, Washington, DC.
[16] J. Yang, X. Jiang, M. Wang, Q. Zhou, R. Chen, J. Optoelectron. Lasers 14 (1) (2003) 12.